行政院國家科學委員會補助專題研究計畫成果報告

※※※※※※※※※※※※※※※※※※※※※※※※※
※ ※
※ ※
※ 砷化銦自聚式量子點內應力鬆弛效應與材料交互 ※
※ 產生的電性缺陷的影響 （3/3） ※
※ ※
※※※※※※※※※※※※※※※※※※※※※※※※※

計畫類別： 個別型計畫

計畫編號：NSC 96-2112-M-009-004-

執行期間： 96 年 08 月 01 日至 97 年 07 月 31 日

執行單位： 國立交通大學電子物理學系(所)

計畫主持人： 陳振芳

報告類型： 完整報告

處理方式： 本計畫可公開查詢

中 華 民 國 97 年 10 月 29 日

行政院國家科學委員會補助專題研究計畫

■ 成果報告
□期中進度報告

砷化鎵氮/砷化鎵量子井在應變與鬆弛狀態下的電性研究

計畫類別：■ 個別型計畫 □ 整合型計畫

計畫編號：NSC 96-2112-M-009-004-

執行期間： 96 年 08 月 01 日至 97 年 07 月 31 日

計畫主持人：陳振芳

共同主持人：

計畫參與人員：

成果報告類型(依經費核定清單規定繳交)：□精簡報告 ■完整報告

本成果報告包括以下應繳交之附件：

□赴國外出差或研習心得報告一份

□赴大陸地區出差或研習心得報告一份

□出席國際學術會議心得報告及發表之論文各一份

□國際合作研究計畫國外研究報告書一份

處理方式：除產學合作研究計畫、提升產業技術及人才培育研究計畫、列管計畫及下列情形者外，得立即公開查詢

□涉及專利或其他智慧財產權，□一年□二年後可公開查詢

執行單位：國立交通大學

中 華 民 國 97 年 10 月 29 日

目錄

目錄 …… 3

中文摘要 …… 4

英文摘要 …… 5

前言 …… 6

研究目的 …… 6

研究方法 …… 6

結果與討論 …… 6

參考文獻 …… 8

計畫成果自評 …… 9

圖 …… 10

表 …… 17

附錄 …… 18

中文摘要

本研究方法主要是藉由光性及電性的量測，包括光激發螢光頻譜(PL)、電容電壓(C-V)、導納頻譜(C-F&G-F)、深層能階暫態頻譜儀(DLTS)及暫態電容(transient)的量測、還有 TEM 表面分析技術，來探討 InAs/InGaAs 這種 DWELL 結構的量子點在應力鬆弛後所展現的特殊現象，主要著重在量子躍遷機制的改變。並將樣品予以熱退火 650℃和 700℃ 1 分鐘作為進一步研究。由 TEM 得知因為量子點成長超過臨界厚度，量子點內部及底層產生差排缺陷。而 DLTS 的量測顯示此缺陷捕捉載子濃度小於 TEM 觀測到的缺陷濃度及量子點濃度，表示缺陷不足以完全空乏量子點中的電子；與未應力鬆弛的樣品比較下，前者的 PL 頻譜在低溫仍有很明顯量子點訊號存在，顯示應力鬆弛並未完全破壞量子點特性。在量子點區域附近隨著偏壓的加深，C-F 高溫量測到活化能越大表示載子分別依序由激發態和基態放射，而 C-V 量測也估算出載子至少填滿到第一激發態的量子能階。C-F 的分析顯示：電子躍遷在高溫是熱激發跳躍，而低溫載子以穿遂形式出去。由低溫穿遂時間計算所擬合的能障與高溫活化能相近，表示載子在高溫是直接跳上 GaAs 導帶的法。將熱退火處理樣品的比較發現底層缺陷產生之空乏效應仍存在，影響著 C-V 與 C-F 的量測結果。由 C-F 量測結果得知，熱退火會減低低溫穿遂時間與高溫活化能，與 PL 藍移結果相符，證實 C-F 量測的來源是量子訊息。

關鍵詞：量子點、應力鬆弛、電子放射

Abstract

We investigate the properties of strain relaxed InAs/InGaAs dot-in-well (DWELL) quantum dots (QDs) by optical and electrical measurement. This research emphasizes the mechanism of the electron emission from the QDs containing a misfit defect state. The QD samples are grown by molecular beam epitaxy (MBE) with and without rapid thermal annealing (RTA). Strain relaxation is observed to introduce misfits in the QD and neighboring GaAs bottom layer. The DLTS spectra show the concentration of the defect state is not high enough to completely deplete the electrons in the QD states. Besides, the photoluminescence quality for relaxed sample is comparable to that of the non-relaxed sample, and the quantum emission (Q.E.) in the relaxed sample can be measured, suggesting that relaxation doesn't degrade the QD. From C-F measurements, electron emission from the relaxed sample exhibits a relatively long emission time with a very broad energetic spectrum due to the depopulation of the QD first excited and ground states. Moreover, from the area under the peak of the depth profiles, electrons are filled up at least to the QD first excited state. From C-F analysis, electron emission from the QDs show a thermal emission at high temperatures, and the tunneling emission prevails at low temperature. The energy barrier height evaluated from the tunneling time is consistent with the thermal emission energy which also agrees with the formula for the tunneling barrier versus tunneling time, suggesting that electrons are thermally activated from the QD states to the GaAs conduction band. The results of the C-V and C-F show that the effect of tunneling suppression due to the additional carrier depletion still exists after annealing 650℃ and 700℃. RTA is found to decrease the electron-emission time and emission energy, consistent with the optical blue-shift due to the inter-diffusion of atoms across the QD interface.

Keyword: quantum dot、strain relaxation、electron emission

前言

研究應力鬆弛的結構，最原始的目的是為了減緩晶格間的不匹配、拉長量子點波長、以及成長更均勻更高密度的量子點。但結果發現此結構，在量子點成長厚度超過其臨界值後，因為上方 InGaAs（緩衝層）的存在，導致應力鬆弛所產生的差排缺陷，只在 InAs 內部及下方產生，而在上方並無產生缺陷。隨著逆偏及空乏區的加大，下方缺陷造成的載子空乏區，會影響載子經量子點穿遂出去的效應，使得原本極快的穿遂效應而量測不到的量子訊號得以被觀察到。一般量子點在室溫時，穿遂時間約在 ps 等級，受限於儀器而無法測量；但應力鬆弛樣品在室溫下，受到缺陷空乏的影響，已經不再以穿遂主導，反而以熱放射直接跳到 GaAs 導帶為主要方式，而低溫下亦可量到的穿遂時間，整個載子躍遷的機制便改變了，所以藉著調變空乏區，控制穿遂時間，可做為記憶元件的儲存、讀寫以及抹除等應用。因為應力鬆弛所形成的特性，使我們能突破以前所無法量測的量子訊息。

研究目的

我們量測應力鬆弛的樣品與未應力鬆弛樣品比較，應力鬆弛的樣品所量測的載子濃度遠小於TEM所看到的量子點數目。因此多數的電子並未因應力鬆弛所造成的缺陷所空乏。本研究藉由電性、光性量測與模擬計算來推論出應力鬆弛下的樣品中，電子隨溫度變化時的放射行為有熱放射與穿遂兩機制，並進一步將樣品熱退火後量測，驗證出C-F所量測的到訊號來自於量子點而非應力鬆弛下的缺陷。

研究方法

本研究使用分子束磊晶（MBE）法在 n^+-GaAs（100）基板上成長 InAs QDs。長晶溫度 485 ~ 500^0C、成長步驟為先在 substrate 上成長一層 0.2μm GaAs bufferlayer，之後再成長 InAs QD 3.3 ML，接著再長 60 Å InGaAs QW 蓋在 QD 上面，長完 QW 之後再長 20 秒的 LT（500℃）GaAs，最後再覆蓋 0.2μm GaAs cap layer，buffer layer 及 cap layer 摻雜矽濃度為 10^{17} cm^{-3}。為了做電性量測，在樣品上蒸鍍 Al 來形成 schottky diodes。

樣品的電性量測是利用Al所形成的schottky contact（陽極）及In所形成的ohmic contact（陰極）並使用HP4194A 阻抗/增益相位分析儀分析C-V (capacitance-voltage)及C-F (capacitance-frequency)頻譜。PL頻譜量測是使用532 nm的固態雷射激發樣品所測量到。深層能階暫態頻譜量測（DLTS）則是利用脈衝產生器、雙閘訊號平均器、電容計所構成的。

結果與討論

由圖 1 的 TEM 分析技術證明了此樣品的插排缺陷存在於量子點內部與底層 GaAs 處。另外，圖 2 為固定 rate window 2.15 ms，偏壓範圍在-1.3 V ~ -2.3 V，變換不同 filling pulse，對樣品做的 DLTS 量測，量測結果此缺陷是屬於會飽和的缺陷，利用其飽和峰值 $\Delta C = 0.3$ pF，經由理論計算公式 $N_T = N_D(\Delta C/C_o^2)$ A，得到捕捉載子而被 DLTS 量測到的缺陷濃度 N_T 約為 2.35×10^9 cm^{-2}，其中樣品參雜濃度 $N_D = 1\times10^{17}$ cm^{-3}、初始電容值 C_o = 270 pF、本樣品介電常數 = 1.14×10^{-10} F/m、金屬接面量測面積 $A = 5\times10^{-3}$ cm^2，將此

缺陷濃度 2.35×10^{9} cm^{-2} 與量子點濃度 $3\sim5\times10^{10} cm^{-2}$[1]比較後，顯示此缺陷捕捉載子濃度小於量子點濃度，說明此樣品中的缺陷還不足以完全空乏量子點中的電子[2]。因此，應力鬆弛的量子點樣品仍有量子躍遷訊號可被量測。

圖 3 (a)與(b)分別是有無應力鬆弛樣品在低溫與室溫的 PL 比較,(a)圖在低溫 50K 下顯示：應力鬆弛下的樣品在光性上仍有不錯的載子侷限性，所以應力鬆弛後 PL 特性並不會比未鬆弛的樣品差，表示 QD 的量子特性仍然存在。低溫與室溫都可看出 PL 峰值的波長有藍位移(blue-shift)的現象，如圖中箭頭所示。圖(b)室溫下 PL，應力鬆弛下的樣品發光強度明顯比未應力鬆弛樣品弱，是由於應力鬆弛後波長藍位移，對應 QD 中的能階抬升，所以侷限載子能力變差，而且又由於溫度上升導致載子有較高的熱能、容從量子點中逃脫，因此發光效率會很明顯變低[3]，而低溫時應力鬆弛下的 QD 的載子侷限性不差是不容置疑的。

圖 4 為樣品有無熱退火時的 C-V 量測與縱深分佈圖；在 C-V 量測中，偏壓於2 V ~ 3V 左右及未端的大偏壓下都有平台的現象，表示此處有載子堆積的情形，而小偏壓有頻率響應的平台是因為所侷限載子躍遷的頻率在高頻時會趕不上，已經失去原本正常 QD 所有頻率皆可趕上的躍遷特性。隨著熱退火溫度升高，平台起始偏壓也較早，較早掃到 QD[4, 5]，合理以量子侷限解釋；熱退火使量子能階提升，侷限載子能力變弱，致使偏壓較早掃到 QD 處，且平台較短，載子累積在 QD 較少。在縱深分佈圖，顯示在 QD 位置約 0.2 m 左右(電性量測容易受到樣品電阻或漏電流影響，QD 位置些許偏移)有隨頻率消長的 peak，表示載子在高頻有跟不上量測頻率的現象，躍遷的速率並不像量子躍遷快，而趕不上頻率的載子在之後的空乏區中被 DC bias 掃出，之後量測結果都顯示此訊號為量子躍遷的說法，而樣品中存在的缺陷正是影響量子躍遷的主因。訊號尖峰位置往後移是由於串聯電阻效應，而且缺陷捉住自由載子除了造成後面產生一大範圍的空乏區外，在 0.35 m 左右也出現缺陷訊號，載子濃度急遽上升。

在 C-V 量測所看到的電容平台及頻率響應的現象，因此進一步在此偏壓範圍進行 C-F 導納頻譜量測，再經由 C-F 量測所繪之 Arrhenius plot，如圖 5，每個偏壓都將會得到多組頻率的 C-F 反曲點配合量測的溫度，來探討此區域的載子躍遷情形。C-F 量測所繪之 Arrhenius plot 中，可區分為高溫與低溫兩部份，差別只在斜率與截距的不同，高溫部份與一般量測所見之 Arrhenius plot 分析相同，可針對不同偏壓以公式求出活化能及捕捉截面積，結果列於表 1 中，三片樣品皆有活化能隨著偏壓的深入而升高的趨勢，就載子被侷限的整體區域範圍來看：活化能有隨著熱退火溫度升高而變小的趨勢，與熱退火對量子點的影響相符，量子能階的抬升初步顯示 C-F 所量測到的量子訊號。捕捉截面積相較於 DLTS 量測到的缺陷訊號稍小，也隨偏壓加大造成的電場變化而改變，在下節將進一步分析；而低溫部份則斜率轉為負值，已無跳躍而上的活化能。

為了更進一步探討載子的躍遷機制，我們藉由之前 C-F 的量測數據，首先對三片樣品做躍遷時間對溫度倒數關係圖，如圖 6 所示，其中縱軸取對數以方便分析。而 emission rate 可由兩部分組成，即 $e_n=e_{tun}+e_{th}$ [6]，其中 e_{tun} 為低溫的穿遂率[7]，而 eth 則為熱激發率，分別由以下公式表示：

$$e_{th}(T,F) = \gamma T^2 \sigma_n \exp[-\frac{Ea}{kT}] \qquad (1)$$

$$e_{tun} = \frac{qF}{4\sqrt{2m^* E_h}} \exp[-\frac{4}{3}\frac{\sqrt{2m^* E_h{}^3}}{q\hbar F}] \qquad (2)$$

對 n-type GaAs，為 $2.28\times10^{20}cm^{-2}s^{-1}K^{-2}$ (與溫度無關的常數)、F 為電場、E_h 為穿遂能障(tunneling barrier height)。圖 6 很清楚說明高溫時載子熱激發而上，溫度下降後慢慢轉為時間固定的穿遂現象，低溫又大偏壓下會因為穿遂時間過長儀器無法量測。我們利用上面提到的公式，以及 Mathematica 繪圖軟體，針對圖 6 數據來擬合，結果如圖 7，其中電場是以金半接面結構的理論來計算，普遍約在 10^6 V/m 的等級，小偏壓下擬合結果與實驗數據是符合的，但有些偏壓溫度轉折處也許因載子躍遷機制並非如此單純，所以擬合結果較不符合。將低溫穿遂時間的數據帶入(2)式後，所求得之 tunneling barrier height E_h 與高溫 C-F 量測所求得之活化能數據相去不遠，表示此為高低溫不同機制的量子躍遷：高溫時載子有足夠熱能跳上導帶，而低溫則以穿遂現象為主。因此藉由不同偏壓量測之高溫活化能數據，帶入低溫穿遂公式，以彌補實驗上無法量測低溫大偏壓的不足，求得低溫穿遂的時間。大體看來，偏壓由大到小，穿遂時間由 10-3 s ~ 10-6 s，分別是由基態與激發態穿遂出去，且隨熱退火溫度上升導致的能階提升，時間些微減小，但等級是差不多的，也與文獻上低溫 40 K 下量子躍遷時間~10 ms 數量級差不多[8]。接著參考其他文獻進一步去分析。首先在高溫熱激發公式(1)中的捕捉截面積 σ_n 有以下關係式[9]：

$$\sigma_n = \sigma_{F=\infty} \exp[-\frac{4}{3\hbar Fq}\sqrt{2m^* E_B^3}] \qquad (3)$$

$\sigma_{F=\infty}$ 是與電場無關的捕捉截面積，E_B 為載子穿遂前所見之三角形狀的能障(triangular barrier)，將(4-3)式做簡單的數學運算後，改為下面形式：

$$\ln\sigma_n = \ln\sigma_{F=\infty} - \frac{1}{F}\frac{4}{3\hbar q}\sqrt{2m^* E_B^3} \qquad (4)$$

再利用表 1 中 C-F 高溫量測求得不同偏壓下的捕捉截面積，取對數後對電場倒數做圖 8，則可以用直線擬合出能障 E_B 及 $\sigma_{F=\infty}$ ，所求分別為 As grown 的 $E_B = 5.97\times10^{-6}$ meV、$\sigma_{F=\infty} = 2.98\times10^{-16}cm^2$ ，及熱退火 650℃的 $E_B = 3.44\times10^{-6}$ meV、$\sigma_{F=\infty} = 2.22\times10^{-16}cm^2$，一般量子躍遷都先往上跳躍再穿遂的兩階段式躍遷[5, 10]，所以會有穿遂能障 E_B，如圖 8 插於右上之能帶示意圖，文獻上以(4)式算法估計出的能障約為 48 meV[10]，但 relaxed 樣品估出之 E_B 小到幾乎可忽略，因此可說載子高溫幾乎無穿遂現象。另外將低溫穿遂時間對 C-F 量測之高溫活化能做圖，如圖 9 所示，考慮(2)式，其低溫的穿遂率受 tunneling barrier height E_h 的影響較電場大，因此若不考慮電場的變數，可用(2)式擬合圖 9 的數據，且大致符合，因此也可說明其低溫的 tunneling barrier height E_h 與高溫活化能 E_a 是相對應的。由以上皆證明了載子高溫直接上跳至導帶的說法。

參考文獻

[1] 蕭茹雄,交通大學電子物理研究所博士論文, ”分子束磊晶法於砷化鎵基板製作 1.3

微米半導體雷射” (2005)
[2] F. Chen et al., “Relaxation-induced lattice misfits and their effects on the emission properties of InAs quantum dots”, Nanotechnology, **18**, 35 (2007)
[3] 陳宜屏,交通大學電子物理研究所碩士論文, ”氮含量與砷化銦厚度對砷化銦/砷化鎵量子點光性影響” (2003)
[4] C. M. A. Kapteyn et al., “Hole and electron emission from InAs quantum dots”, Appl. Phys. Lett. **76**, 1573 (2000)
[5] C. M. A. Kapteyn, F. Heinrichsdorff, O. Stier, R. Heitz, M. Grundmann, N. D. Zakharov, and D. Bimberg, “Electron escape from InAs quantum dots”, Phys. Rev. B **60**, 14265 (1994)
[6] J. Iba´n˜ez, R. Leon, D. T. Vu, S. Chaparro, S. R. Johnson, C. Navarro, and Y. H. Zhang, “Tunneling carrier escape from InAs self-assembled quantum dots”, Appl. Phys. Lett. **79**, 2013 (2001)
[7] E. N. Korol et al., “Ionization of impurity states in semiconductors by an electric field”, Sov. Phys. -Solid State, **19**, 1327 (1977)
[8] C. M. A. Kapteyn et al., ”Carrier emission processes in InAs quantum dots”, Physica E, **7**, 388 (2000)
[9] M. Geller et al., ”Hole capture into self-organized InGaAs quantum dots”, Appl. Phys. Lett. **89**, 232105 (2006)
[10] W. -H. Chang et al., “Hole emission processes in InAs/GaAs self-assembled quantum dots”, Phys. Rev. B, **66**, 195337 (2002)

計畫成果自評

經過三年的研究雖然能有部分現象並未能得到解答，但在應力鬆弛下所產生的效應已經研究出，並得以利用理論與實驗雙方面同時驗證。我們也將研究成果投稿至nanotechnology 與 Journal of Applied Physics。所幸在去年時前者已被接受且發表(附錄)；而後者則是近期投出，因此仍在審理。對於計畫成果我們相信仍還可以在進一步的探究我們未解決的現象，使得此研究能盡善盡美，最後我們自評優良算是給予我們團隊鼓勵。

圖.

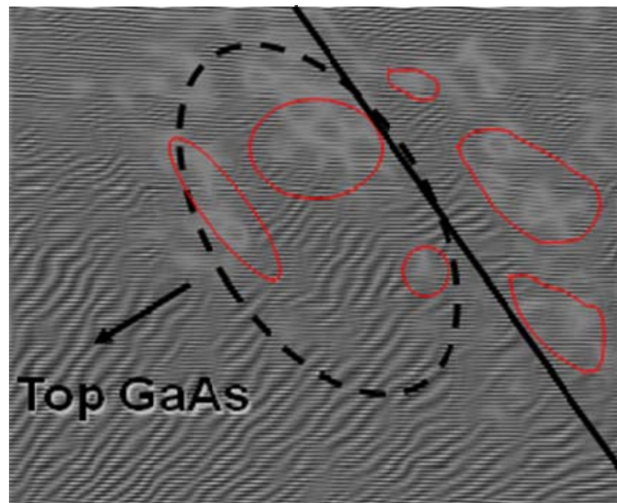

Fig. 1 relaxed 樣品經 TEM 量測並傅立葉轉換於量子點附近。

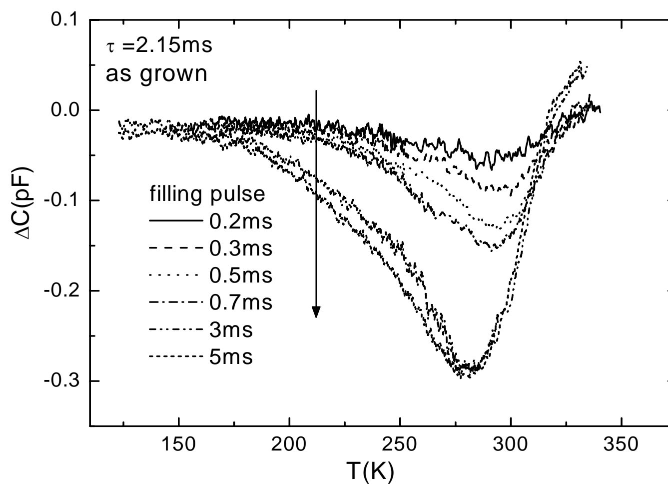

Fig. 2 固定 rate window 2.15 ms，偏壓範圍在-1.3 V ~ -2.3 V，變換不同 filling pulse，對 relaxed 樣品做的 DLTS 量測。

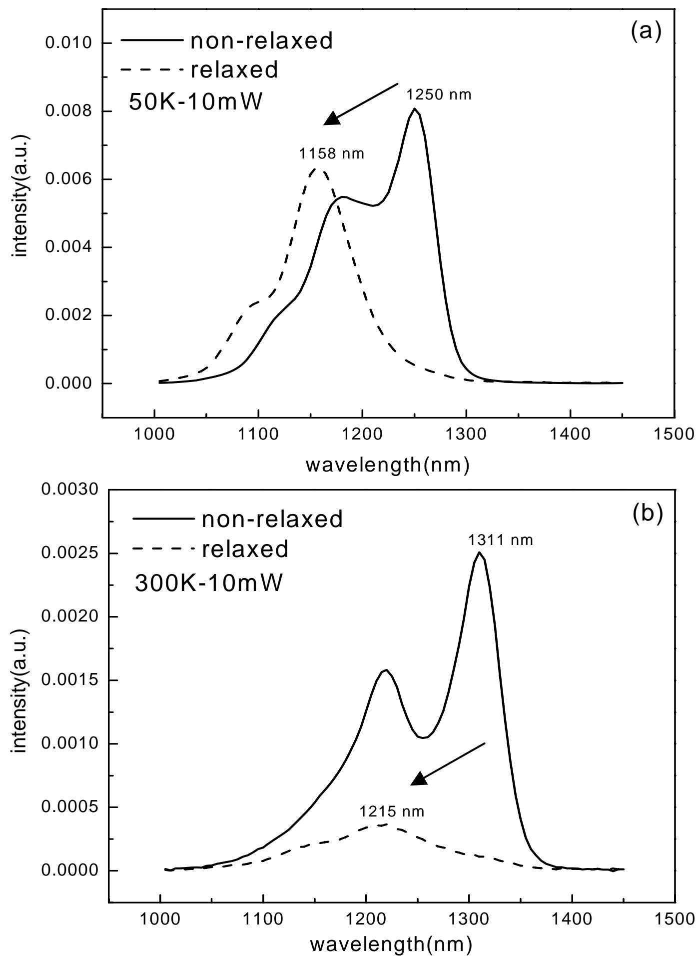

Fig. 3(a), (b) 分別是 non-relaxed 與 relaxed 樣品在低溫 50K 與室溫 300K 的 PL 比較。

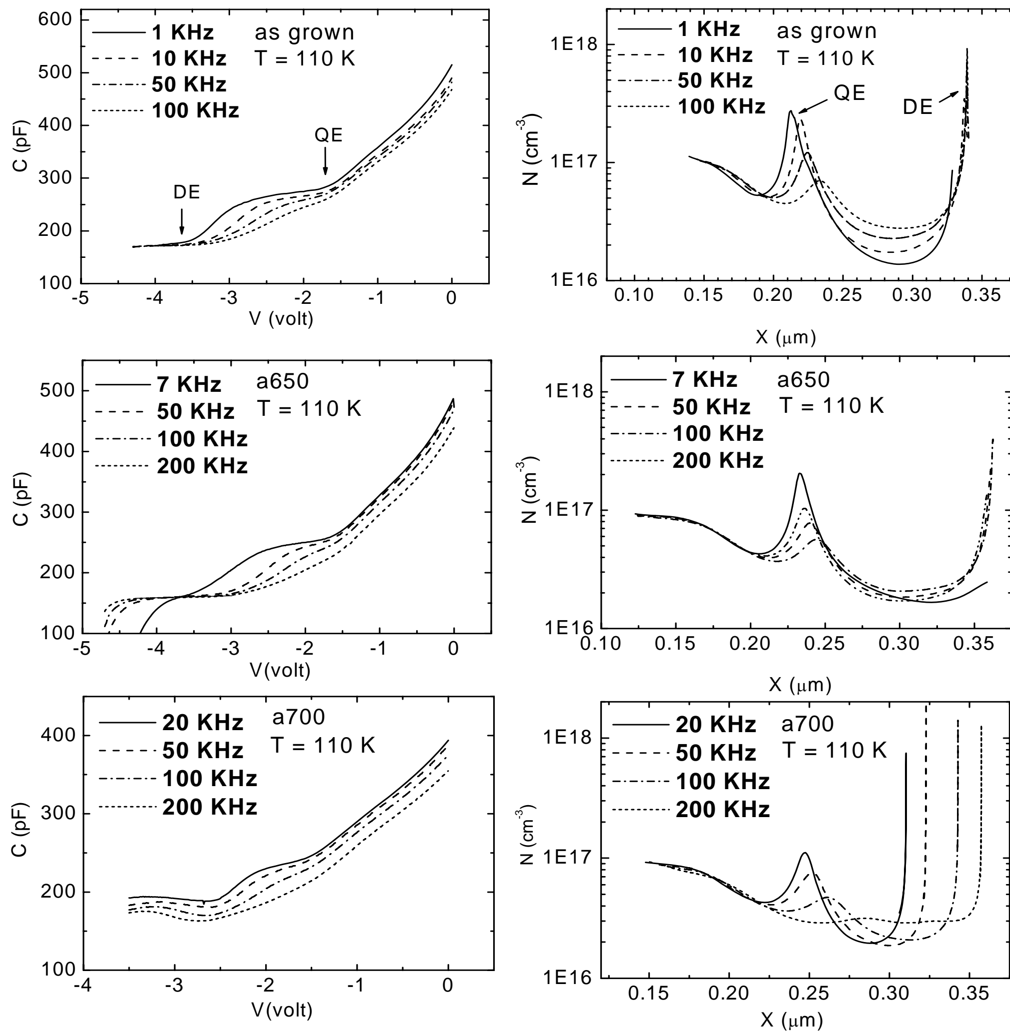

Fig. 4 為 relaxed 樣品 as grown 與熱退火 650℃及 700℃低溫 110K 下不同頻率的 C-V 圖，與經由其轉化的縱深分佈圖。

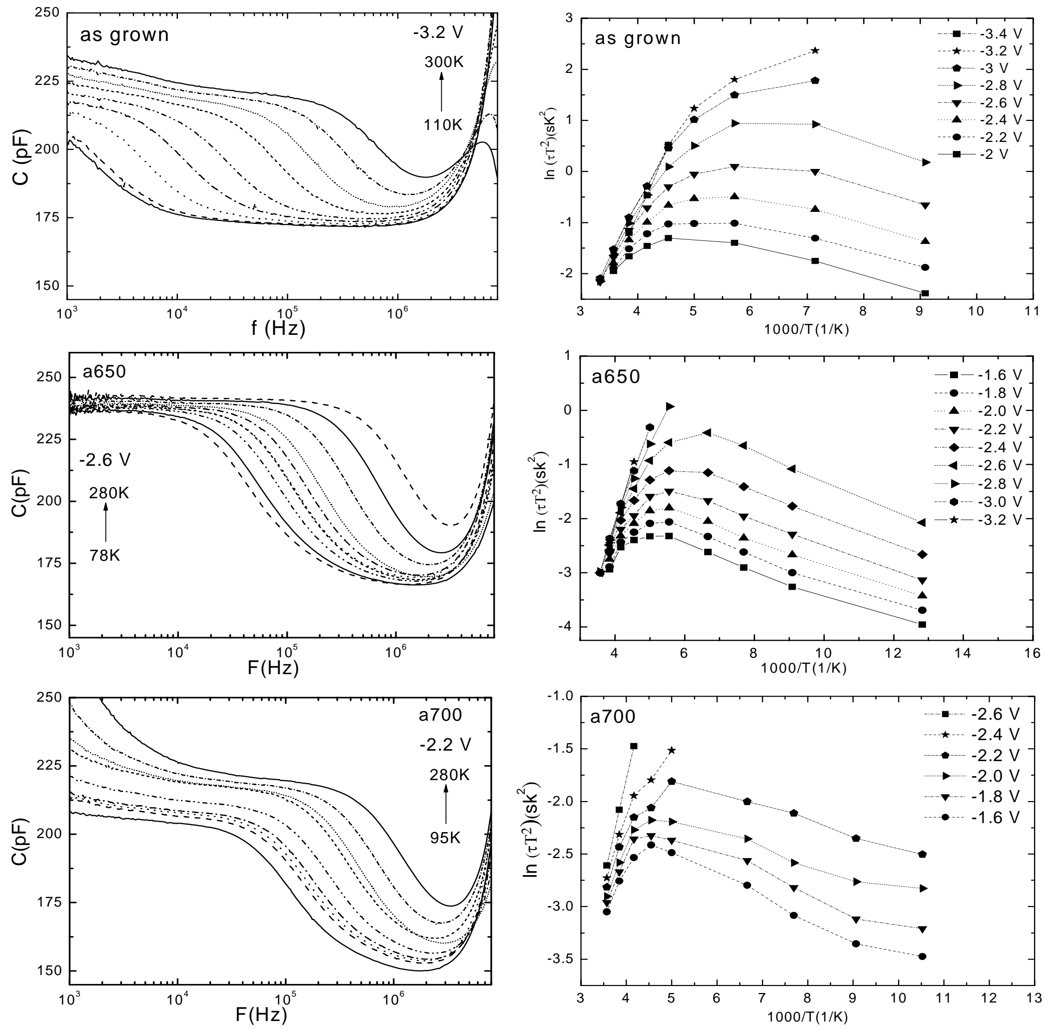

Fig. 5 為 relaxed 樣品 as grown 與熱退火 650℃及 700℃在偏壓分別為-3.2、-2.6、-2.2 V 下不同溫度的 C-F 圖，及經由 C-F 量測所繪之 Arrhenius plot。

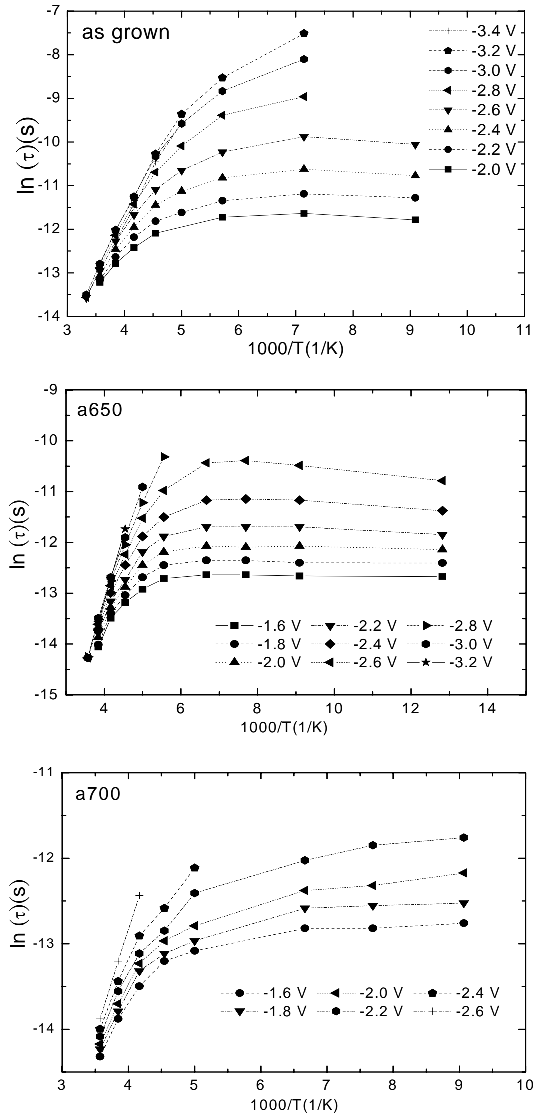

Fig. 6 為 relaxed 樣品 as grown 與熱退火 650℃及 700℃的 C-F 量測之躍遷時間對溫度關係。

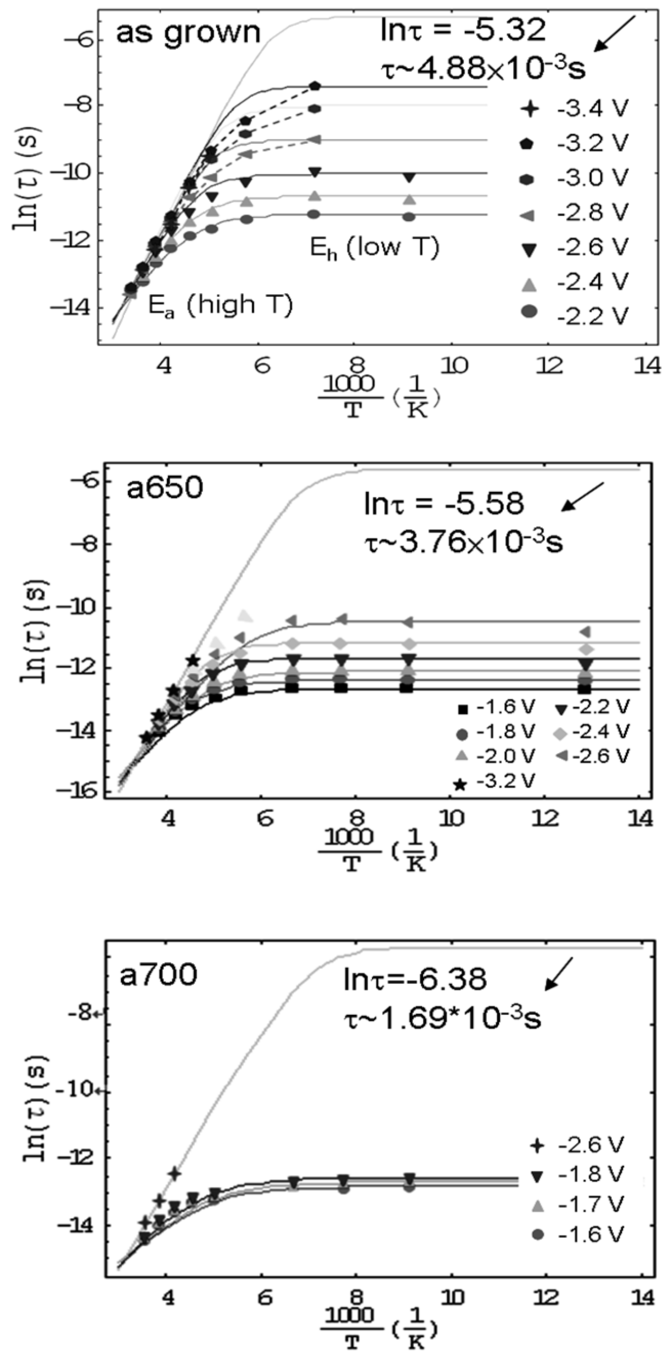

Fig. 7 為 relaxed 樣品 as grown 與熱退火 650℃及 700℃的 C-F 量測載子躍遷之公式擬合

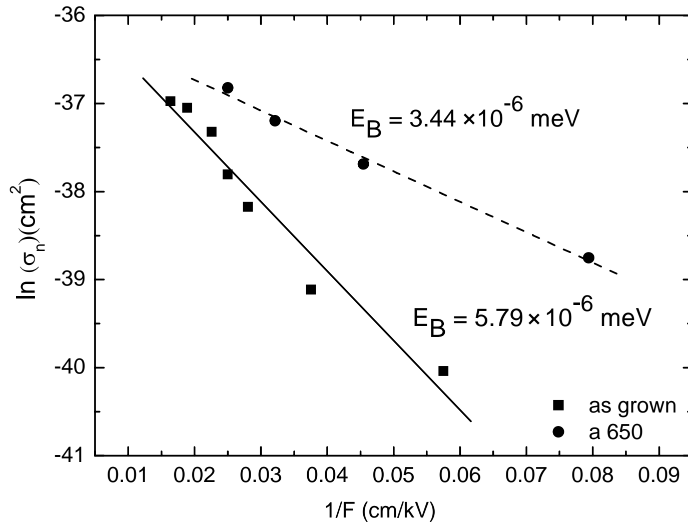

Fig. 8 為 relaxed 樣品 as grown 與熱退火 650℃的捕捉截面積對電場倒數關係

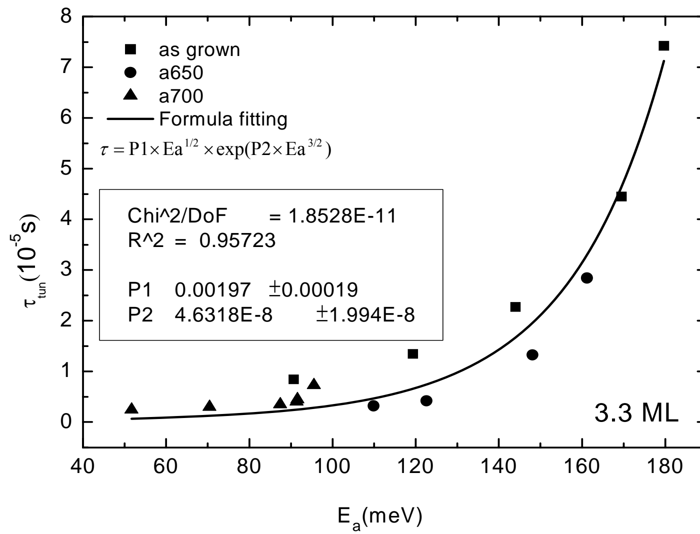

Fig. 9 為 relaxed 樣品 as grown 與熱退火 650℃及 700℃的穿遂時間對活化能關係與公式擬合。

表.

表 1. relaxed 樣品 as grown 與熱退火 650℃及 700℃三片的 C-F 分析之活化能與捕捉截面積

3.3 ML As grown			3.3 ML Anneal 650℃			3.3 ML Anneal 700℃		
Bias (V)	**Ea** (meV)	**Capture Cross section** (cm^2)	**Bias** (V)	**Ea** (meV)	**Capture Cross section** (cm^2)	**Bias** (V)	**Ea** (meV)	**Capture Cross section** (cm^2)
-2	90.64	1.97×10^{-20}	-1.3	86.3	2.81×10^{-18}	-1.5	51.67	2.91×10^{-19}
-2.2	119.35	4.09×10^{-18}	-1.4	92.77	3.66×10^{-18}	-1.7	70.42	1.56×10^{-18}
-2.4	144.03	1.03×10^{-17}	-1.6	109.87	1.11×10^{-17}	-1.8	87.45	3.15×10^{-18}
-2.6	169.47	2.64×10^{-17}	-1.8	122.61	1.87×10^{-17}	-2.0	91.60	3.51×10^{-18}
-2.8	191.56	6.18×10^{-17}	-2.2	122.61	1.48×10^{-17}	-2.2	95.53	3.72×10^{-18}
-3.0	200.27	8.11×10^{-17}	-2.4	148.10	4.29×10^{-17}	-2.4	112.78	7.02×10^{-18}
-3.2	201.88	8.75×10^{-17}	-2.6	161.21	7.00×10^{-17}	-2.6	164.30	5.36×10^{-17}
-3.4	212.74	1.96×10^{-16}	-2.8	171.22	1.02×10^{-16}			
			-3.0	184.92	1.84×10^{-16}			
			-3.2	192.71	2.78×10^{-16}			

附錄

IOP PUBLISHING NANOTECHNOLOGY

Nanotechnology 18 (2007) 355401 (7pp) doi:10.1088/0957-4484/18/35/355401

Relaxation-induced lattice misfits and their effects on the emission properties of InAs quantum dots

J F Chen[1], Y Z Wang[1], C H Chiang[1], R S Hsiao[1], Y H Wu[2], L Chang[2], J S Wang[3], T W Chi[4] and J Y Chi[4]

[1] Department of Electrophysics, National Chiao Tung University, Hsinchu, Taiwan, Republic of China
[2] Department of Materials Science and Engineering, National Chiao Tung University, Hsinchu, Taiwan, Republic of China
[3] Department of Physics, Chung Yuan Christian University, Chung-Li, Taiwan, Republic of China
[4] Industrial Technology Research Institute (OES/ITRI), Hsinchu, Taiwan, Republic of China

E-mail: jfchen@cc.nctu.edu.tw

Received 25 April 2007, in final form 10 July 2007
Published 7 August 2007
Online at stacks.iop.org/Nano/18/355401

Abstract
Strain relaxation in InAs/InGaAs quantum dots (QDs) is shown to introduce misfits in the QD and neighboring GaAs bottom layer. A capacitance–voltage profiling shows an electron accumulation peak at the QD with a long emission time, followed by additional carrier depletion caused by the misfits in the GaAs bottom layer. The emission-time increase is explained by the suppression of tunneling for the QD excited states due to the additional carrier depletion. As a result, electrons are thermally activated from the QD states to the GaAs conduction band, consistent with observed emission energies of 0.160 and 0.068 eV which are comparable to the confinement energies of the QD electron ground and first-excited states, respectively, relative to the GaAs conduction band. This is in contrast to non-relaxed samples in which emission energy of 60 meV is observed, corresponding to the emission from the QD ground state to the first-excited state.

1. Introduction

Recently, InAs/GaAs self-assembled quantum dots (QDs) [1–5] have attracted considerable attention because of their promising technological applications [6–8] and for scientific studies [9–13]. One of the important issues is experimentally determining the electronic band structure of the QD [9–14]. Kapteyn *et al* [9] have proposed a two-step emission process for electrons in the QD: a thermal activation from the QD ground state to the first-excited state and then tunneling to the GaAs conduction band. This suggests a strong tunneling for electrons emitting from the QD excited states. Since the tunneling probability can be affected by varying the depletion width, introducing additional carrier depletion may suppress the tunneling process and enable the observation of the thermal emission from the QD ground state to the GaAs conduction band. Coherent QDs can be formed by partial strain relaxation. However, when the InAs thickness is increased beyond the critical thickness (~3 ML), the strain is relaxed by generating misfit dislocations [13]. Uchida *et al* [15] have observed a perfect confinement of misfit dislocations at the relaxation interface in InGaAs/GaAs heterostructures. In previous work [14], misfit dislocations were shown to be electron-trapping centers. The misfits in the bottom GaAs layer may cause carrier depletion and suppress the tunneling probability. This may significantly modify the emission properties of the QD. Therefore, in this work, the relaxation-induced misfit dislocations and their effects on the electron emission in InAs QDs are investigated by transmission electron microscopy (TEM), capacitance–voltage (C–V) profiling and deep-level-transient spectroscopy (DLTS).

The samples studied are InAs QDs capped with an InGaAs layer. With this capping layer, relaxation-induced misfit

 © 2007 IOP Publishing Ltd Printed in the UK

dislocations are found in the QD and neighboring GaAs bottom layer. The carrier depletion caused by the misfit dislocations in the neighboring GaAs bottom layer can suppress the electron emission from the QD excited states, leading to a longer emission time and larger emission energy. Evidence of this tunneling suppression is provided by another QD sample without an InGaAs capping layer. Strain relaxation does not produce misfit dislocations in the bottom GaAs layer. Without additional carrier depletion behind the QD, the emission time remains very short.

2. Experiments

The QD structures were grown on n^+-GaAs(100) substrates by solid source molecular beam epitaxy in a Riber machine. On top of a 0.3 μm thick Si-doped GaAs (6–10 $\times$ 10^{16} cm^{-3}) barrier layer, an InAs layer with different thickness from 2 to 3.3 ML was deposited at 490 °C to form the QDs. Then the QDs were capped with a 60 Å $In_{0.15}Ga_{0.85}As$ layer and a 0.2 μm thick Si-doped GaAs (6–10 $\times$ 10^{16} cm^{-3}) layer to terminate the growth. Detailed growth conditions can be found elsewhere [16]. A typical QD sheet density about 3×10^{10} cm^{-2} was observed by atomic force microscopy (AFM). For C–V profiling, Schottky diodes were realized by evaporating Al on the samples. The apparent-carrier concentration is obtained by converting the C–V curve using the depletion-layer approximation: $N(w) = \frac{C^3}{A^2 q \varepsilon \varepsilon_0 (dC/dV)}$, where W is the width of the space-charge region and A is the contact area. Photoluminescence (PL) measurements were carried out using a double-frequency yttrium–aluminum–garnet (YAG): Nd laser at 532 nm.

3. Measurement and results

3.1. TEM characterization of misfit dislocations

In contrast to there being no dislocations in the non-relaxed samples, misfit dislocations are observed in the relaxed InAs/InGaAs QDs samples. Figure 1(a) shows a large-scale cross-sectional TEM picture of a QD sample with a 3.3 ML thick InAs layer. The QD is relaxed since the InAs thickness exceeds the critical thickness of ~3 ML [13]. A line of QDs is visible. No threading dislocations are observed in the top GaAs layer. Figure 1(b) shows the TEM picture around a dot whose contrast is similar to that of a non-relaxed dot. The shape of the dot looks more like a trapezium with a height ~10 nm and a base width ~20 nm. Figure 1(c) shows a high-resolution TEM picture around a typical dot (dashed ellipse). As a guide to the eyes, the wetting layer is indicated by a line. Figure 1(d) shows the Fourier transformed image of figure 1(c). The area around the GaAs bottom layer near the QD is emphasized in figure 1(e) for clarity. Several (about ten) dislocations, as indicated by loops, can be seen in the QD. No dislocations are found in the intervening GaAs region between adjacent QDs. About eight dislocations are observed in the bottom GaAs layer near the dot: two in each of the two small loops on the sides, and four in the large middle loop. From a dot density of ~3×10^{10} cm^{-2} observed by AFM, the total density of the dislocations is ~5.4×10^{11} cm^{-2} on the average. These dislocations do not propagate into the GaAs layers but

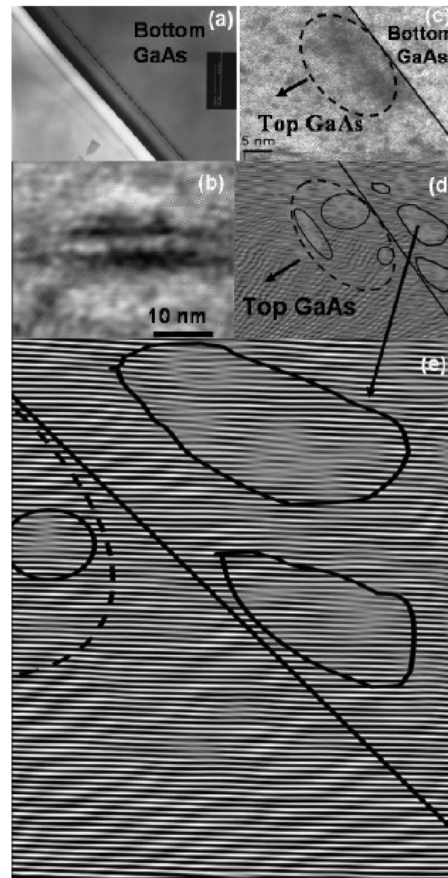

Figure 1. (a) Cross-sectional TEM picture of the 3.3 ML InAs/InGaAs QDs sample, showing a line of QDs and no threading dislocations in the top GaAs layer. (b) The TEM image of a typical QD, showing a height ~10 nm and a base width ~20 nm. (c) The HRTEM picture of a dot (dashed ellipse). As a guide to the eyes, the wetting layer is indicated by a line. (d) The corresponding Fourier transformed image, showing a number of misfit dislocations in the QD and in the neighboring GaAs bottom layer. (e) Part of figure (d), showing more clearly the misfit dislocations in the large middle loop in (d).

are confined near the QD lower interface. Therefore, there are misfit dislocations induced by strain relaxation, rather than threading dislocations generated from the sample surface or substrate through a gliding process. These misfit dislocations bend toward the interface. It should be noted that, besides these misfit dislocations, the sample reveals no other defects. Hence, relaxation-induced misfit dislocations are confined in the QD and neighboring GaAs bottom layer. Similar confinement of misfit dislocations was previously observed in relaxed InGaAs/GaAs heterostructures [15]. This misfit distribution, together with the fact of there being no threading dislocations in the top GaAs layer [17], suggests that strain relaxation occurs at the QD lower interface while the QD upper surface probably remains coherently strained.

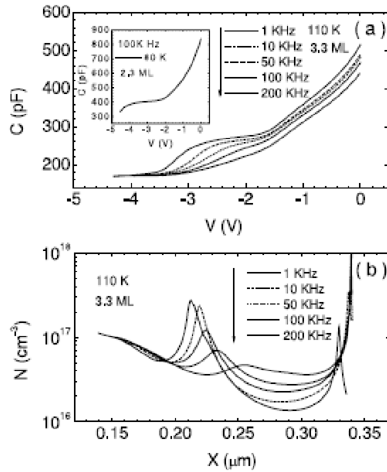

Figure 2. (a) Frequency-dependent C–V spectra and (b) converted concentration profiles of the relaxed 3.3 ML sample, showing carrier accumulation in the dots and additional carrier depletion in the neighboring GaAs bottom layer. The peaks at 0.2 and 0.33 μm are considered as electron emission from the QD and from the traps related to the misfits, respectively. The C–V spectra of the non-relaxed 2.3 ML sample are shown in the inset of (a) for comparison.

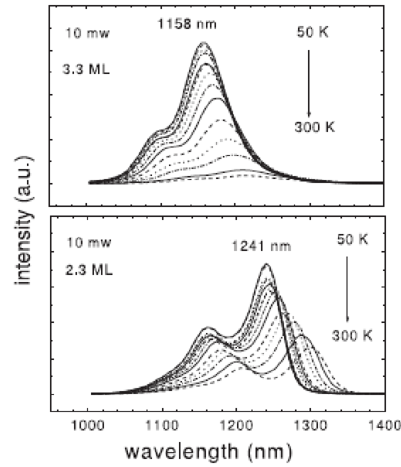

Figure 3. Temperature-dependent PL spectra of the relaxed 3.3 ML and non-relaxed 2.3 ML samples. The QD ground state emits at 1158 nm in the relaxed sample. A relatively strong increase in the linewidth of the QD emission can be seen with increasing temperature.

3.2. Electron emission from a QD

The electron-emission properties of a relaxed QD can be seen from the C–V spectra measured on the 3.3 ML sample. Figures 2(a) and (b) show a C plateau (from -2 to -3 V) and its converted carrier-accumulation peak in the QD region ($\sim$0.2 μm), respectively. The x-coordinate in figure 2(b) is defined as the distance from the sample surface. The intensity of the peak increases with decreasing temperature, characteristic of a Debye-length effect in a quantum structure. The C plateau appears at nearly the same dc voltage as in a non-relaxed 2.3 ML QD sample (in the inset of figure 2(a)), and thus it is ascribed to electron emission from the QD states. The smaller voltage width (from -2 to -3 V) for the C plateau suggests a smaller number of electrons accumulated in the relaxed QD. Hence, some electrons in the QD are depleted by traps presumably associated with the misfits in the QD. It should be noted that the carrier peak at $\sim$0.2 μm cannot be interpreted by the depopulation of the traps associated with the misfits in the QD [14]. Recently, in work on relaxed InAsSb QDs [17], the traps associated with the misfits in the QD were found to emit electrons to the GaAs conduction band with emission energy of 0.35 eV, in a way similar to the misfits in the GaAs layer. Therefore, due to its deeper energy than the QD electron ground state (about 0.18 eV), electron emission from this trap would appear at a much deeper depth than observed. From a simple band diagram simulation, a trap located at 0.2 μm and at 0.35 eV below the GaAs conduction band would appear at about 0.3 μm, rather than the $\sim$0.2 μm observed. Thus, the carrier peak at 0.2 μm is attributed to electron emission from the QD. As shown in figure 2(b), the carrier peak at 0.2 μm is followed by a large peak at around 0.33 μm. Due to the long emission time, the electrons trapped on the misfits would not be modulated by an ac signal but would eventually be swept out when a dc voltage moves the Fermi level well below the related traps. Thus, the large peak at around 0.33 μm is attributed to the electron emission from the misfits. Note that the linewidth of the carrier peak at 0.2 μm is 0.015 μm (at 80 K) which is comparable to that of the non-relaxed sample, suggesting that strain relaxation does not severely degrade the QD. This is supported by the comparable quality for the QD PL emission between the relaxed 3.3 ML and non-relaxed 2.3 ML samples, as shown in figure 3. The PL spectra of the relaxed 3.3 ML sample show a slightly broader QD ground emission at 1158 nm (at 50 K). This suggests the presence of the QD states even after strain relaxation, justifying the assignment of the peak at $\sim$0.2 μm as the emission from the QD states. From the area under this peak in figure 2(b), we estimate a sheet concentration of 1×10^{11} cm^{-2} compared to 4×10^{11} cm^{-3} in the non-relaxed 2.3 ML sample. Thus, the misfits capture some electrons in the QD but do not completely deplete them. For the estimated QD density of 3×10^{10} cm^{-2} from AFM, each QD still contains about three electrons. By comparison with the density of the misfits as shown in figure 1, we deduce that only a small amount of the misfits in the QD are active traps.

By comparison with non-relaxed samples, strain relaxation markedly lengthens the emission time for the QD. This can be seen from the frequency dependence of the C dispersion in figure 2(a). This dispersion is not due to a resistance–capacitance (RC) time constant effect [18], since it is observed in the QD region, rather than in the top GaAs layer except the parallel shift. The RC time constant determined from capacitance–frequency measurements at -0.5 V is about 10^{-6} s and is nearly temperature and voltage independent. The emission time for the QD is much longer than the RC time constant. The high-C plateau of 280 pF in figure 2(a) means that the electrons at the QD can follow an ac signal at

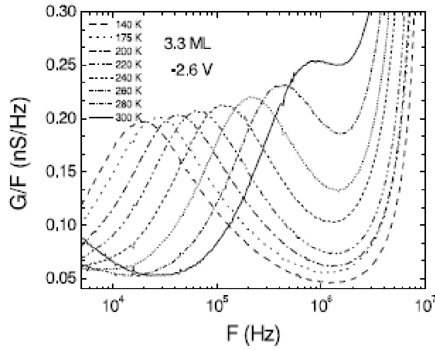

Figure 4. The G/F–F spectra of the 3.3 ML sample measured at −2.6 V, corresponding to the electron emission from the QD. The frequency corresponding to the conductance peak is taken as the carrier emission rate.

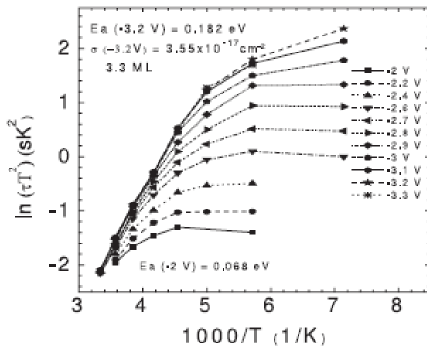

Figure 5. Arrhenius plots of the emission times in the 3.3 ML sample obtained from the G/F–F spectra at different dc voltage. The plots at high temperatures yield emission energy from 0.068 to 0.182 eV from −2 to −3.2 V. The decreased temperature dependence at low temperatures suggests a tunneling effect.

10^3 Hz, but cannot at 2×10^5 Hz, as shown by the low-C plateau of 180 pF. The emission rate is between the two frequencies. By taking the inflexion frequency as the inverse of the emission time, the emission times (at 110 K) are 10^{-5} s at −1.9 V, 2×10^{-5} s at −2 V, 10^{-4} s at −2.2 V, and 10^{-3} s at −2.4 V, respectively. This suggests an increased emission energy as the Femi level is shifted downward. Detailed emission time and energy as a function of voltage are obtained from the conductance/frequency–frequency (G/F–F) spectra, as shown in figure 4 for −2.6 V. The conductance displays a peak at a frequency comparable to carrier emission rate. Figure 5 shows the obtained Arrhenius plots from −2 to −3.3 V. The emission times at high temperatures can be connected by a straight line from which emission energy is obtained, which increases from 0.068 to 0.182 eV from −2 to −3.2 V. Figure 5 shows a decrease in the emission energy with lowering temperature, suggesting some tunneling effect at low temperatures. Since a tunneling effect is usually observed for QDs [9–11], this decreased temperature dependence further supports the assignment of the peak at ∼0.2 μm as the electron emission from the QD states. The highest-bound emission

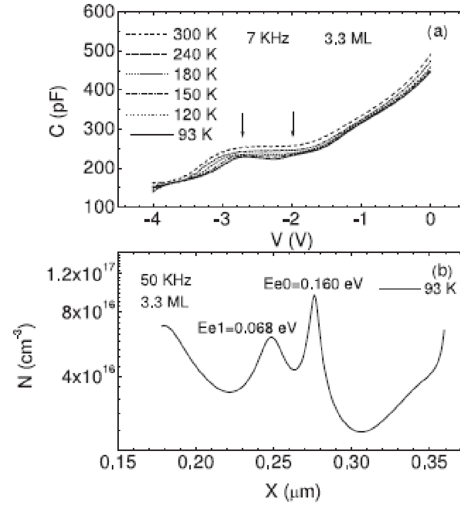

Figure 6. (a) Temperature-dependent C–V spectra and (b) converted concentration profiles at 93 K of the relaxed 3.3 ML sample, showing a splitting of the carrier-accumulation peak into two peaks with emission energies of 0.068 and 0.160 eV related to the electron emissions from the QD electron first-excited and ground states, respectively.

energy of 0.182 eV is comparable to the confinement energy of the QD electron ground state with respect to the GaAs conduction band. Kapteyn *et al* [9] reported a value of 0.190 eV for the confinement energy of the InAs QD ground state for an emission at 1.12 eV which is close to our QD emission at 1.07 eV (at 50 K) in figure 3. Thus, the emission energy 0.182 eV is attributed to a thermal activation from the QD electron ground state to the GaAs conduction band. As regards the lowest-bound emission energy of 0.068 eV, it can be due to the depopulation of the QD first-excited state. As discussed above, from the area under the electron-accumulation peak, each QD contains about three electrons. Thus, the QD is filled up to the first-excited state and electron emission from this state can occur. This is indeed the case. When the temperature is lowered below 120 K, the emissions from the QD electron ground and first-excited states are well separated, as shown in figure 6(a), which shows a splitting of one C plateau into two plateaus, as indicated by arrows. The corresponding electron-accumulation peak also splits into two well-separated peaks, as shown in figure 6(b), which displays the depth profile at 93 K. The peak at 0.25 (0.275) μm corresponds to the QD electron first-excited (ground) state. The smaller peak height for the first-excited state is consistent with the filling of only one electron in the first-excited state, relative to two electrons in the ground state. As illustrated in figure 5, tunneling is unavoidable at low temperatures. The emission energies for these two states are simply estimated from the high-temperature G/F–F spectra at the voltages corresponding to the two C plateaus in figure 6(a), which are 0.068 and 0.160 eV, respectively, as indicated in figure 5. These two values are comparable to 0.086 and 0.177 eV calculated for QDs [19] and 0.096 and 0.190 eV experimentally determined by Kapteyn *et al* [9], and 0.060 and 0.14 eV by Brunkov *et al* [20] from the relative voltage positions of the

C plateaus. This comparability is a good indication that the emission energies of 0.160 and 0.068 eV are the confinement energies of the QD electron ground and first-excited states, respectively, with respect to the GaAs conduction band. Their energy difference (0.092 eV) is comparable to the energy difference between the PL ground and first-excited emissions of the QD, consistent with a very small energy separation between the hole ground and first-excited states [19, 20]. By subtracting the GaAs band gap of 1.50 eV from the electron ground-state energy of 0.160 eV and the ground-state PL emission energy of 1.079 eV (at 50 K), we obtain the confinement energy of the hole ground state to be 0.261 eV, a value close to that of 0.205 eV previously determined by Brunkov *et al* [20]. These results suggest that the observed emission processes (at high temperatures) are from the QD electron and first-excited states to the GaAs conduction band. Thus, the confinement energies of these states with respect to the GaAs conductance band are directly determined from the temperature dependence of the emission times, rather than from the relative voltage positions of the C plateaus which can be strongly affected by the sample resistance. As discussed above, the electron emission from the QD ground and first-excited states can be distinguished when the temperature is lowered to ~120 K. This feature is related to the PL linewidth of the QD ground-state emission in figure 3, which shows a relatively small linewidth of ~60 meV from 50 to 150 K. However, the linewidth increases strongly to ~100 meV when the temperature is increased to 300 K. Since the energy spacing between the ground and first-excited states is only about 0.092 eV, the strongly increased linewidth of the QD ground state would cause the ground and first-excited states to be indistinguishable, consistent with the observation of a single electron-accumulation peak at high temperatures. This comparative study of the PL and the depth profile further confirms that the observed emission is related to the QD states.

So far, we have compared our results with those obtained from capacitance spectroscopy. We now turn to the comparison with the reported data from optical absorption measurements. From intraband absorption, Pal *et al* [21] have reported an energy separation of 0.10 eV between the electron ground and first-excited states for a QD ground emission at 1.19 eV at 77 K, which is very close to our observed value of 0.092 eV. On the other hand, from intraband transmission studies, Adawi *et al* [22] have observed an absorption peak with 0.113 eV due to the transition from the QD electron ground state to the second-excited state. From photocurrent studies, the same authors also reported transitions with 0.17 and 0.22 eV for the transitions from the QD electron ground state to wetting layer and to GaAs continuum states, respectively. Since the lowest-laying state in the wetting layer is at ~50 meV below the GaAs conduction band, we cannot exclude the possibility that our 0.16 eV emission is due to the transition from the electron ground to wetting layer, rather than directly to the GaAs conduction band. If this is true, the QD electron ground state is at about 0.21 eV below the GaAs conduction band edge. This value is more consistent with the analysis by Kim *et al* [23] who claimed that the confinement energy for the QD electron ground state should be larger than 0.19 eV for a QD ground emission at 1.127 eV. Furthermore, based on an argument that the binding energy of the electron ground state is higher than that for the hole ground state, Raghavan *et al* [24] have reported a minimum binding energy of 0.21 eV for the QD electron ground state. These values are all larger than our observed value of 0.16 eV. Thus, there is a possibility that the observed emission processes by time-resolved capacitance spectroscopy is relative to the wetting layer, rather than the GaAs conduction band, leading to a reduction of about 50 meV in the confinement energy. Further investigation on the effect of the wetting layer is needed to make a more conclusive argument on this matter.

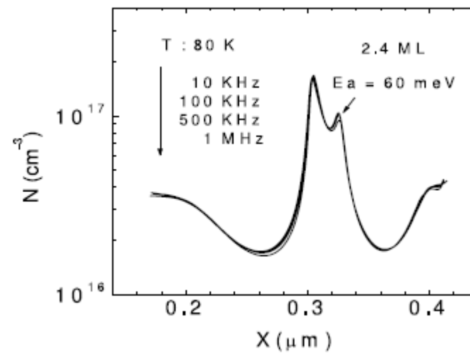

Figure 7. The depth profiling of a non-relaxed 2.4 ML InAs QD sample. The carrier peak at 0.305 μm is attributed to the electrons tunneling from the QD excited states to the GaAs conduction band. The weak peak at 0.325 μm (indicated by an arrow) which shows frequency-dependent dispersion with $Ea = 60$ meV is attributed to a thermal excitation from the QD ground state to the first-excited state.

For comparison, figure 7 shows a typical depth profile for a non-relaxed InAs/InGaAs QD sample with a 2.4 ML thick InAs layer. Detailed discussions on this sample can be found elsewhere [14]. The strong carrier peak at 0.305 μm is attributed to the electrons tunneling [9–11] from the QD excited states to the GaAs conduction band. The emission time is too short to be resolved since no attenuation of this peak is seen up to 1 MHz at 10 K. The weak peak at 0.325 μm (as indicated by an arrow) shows frequency-dependent dispersion whose emission energy is determined to be ~60 meV [14]. Since this energy is comparable to the PL energy spacing between the ground and first-excited peaks, the weak peak is attributed to a thermal excitation from the QD ground state to the first-excited state. After being thermally excited to the first-excited state, the electron subsequently tunnels to the GaAs conduction band, in a two-stage emission process previously described [9]. This shows a marked tunneling effect for the QD excited states in the non-relaxed QD sample.

3.3. Additional carrier depletion due to misfit dislocations

A comparison between figures 2(b) and 7 reveals that strain relaxation considerably lengthens the emission time for the QD. This effect can be explained by the suppression of tunneling due to the additional carrier depletion in the GaAs bottom layer near the QD. Figure 2(b) shows an asymmetrical depth profile with additional carrier depletion in the bottom GaAs layer (0.25–0.32 μm). This depletion has a valley concentration of 1×10^{16} cm^{-3}, compared to that of 5×10^{16} cm^{-3} in the front side of the QD. Furthermore, the width

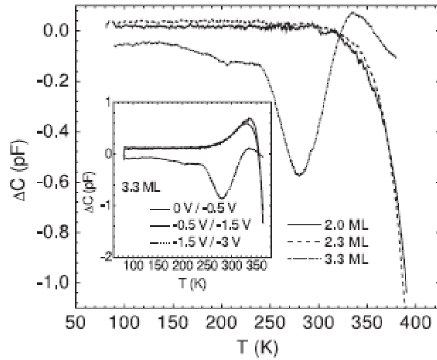

Figure 8. The DLTS spectra at a rate window of 0.86 ms for the non-relaxed 2 and 2.3 ML samples and the relaxed 3.3 ML sample. A trap at 0.35 eV is detected in the 3.3 ML sample for -1.5 V/-3 V, corresponding to the QD and neighboring GaAs bottom layer. The top GaAs layer is free of traps, as is evident from the inset, which shows no trapping signals for 0 V/-0.5 V and -0.5 V/-1.5 V. The continuous broad background signal at low temperatures is thought to be due to the electron emission from the QDs.

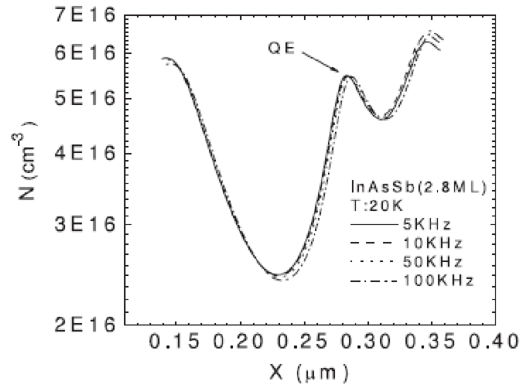

Figure 9. The 20 K depth profile of the 2.8 ML InAsSb relaxed QD sample, showing a weak carrier peak at the QD (indicated by QE) and drastic carrier depletion in the front of the QD. Without the additional carrier depletion in the back of the QD, the emission time for the QD is too short to be resolved even up to 10^5 Hz at 20 K.

of the additional carrier depletion is about 0.1 μm, which is more than three times broader than that in the front side of the QD. Since carriers are emitted to the bottom GaAs electrode, such a broad depletion layer in the back of the QD would significantly reduce the tunneling probability. As a result, the electrons in the QD ground state would have to be thermally activated to the GaAs conduction band. This is consistent with the observed emission energy of 0.160 eV, which is close to the energy spacing between the QD ground state and the GaAs conduction band, in contrast to the observed emission energy of 60 meV for activation from the QD ground state to the first-excited state in the non-relaxed sample.

In view of the TEM data, the misfit dislocations in the bottom GaAs layer can be the reason for the additional carrier depletion. Due to the long emission time, the related traps are revealed by the DLTS spectra as shown in figure 8 for a rate window of 0.86 ms. In contrast to there being no traps in the non-relaxed 2 and 2.3 ML samples, the relaxed 3.3 ML sample displays a trap around 275 K for the sweeping voltage of -1.5 V/-3 V, corresponding to the QD and neighboring GaAs bottom layer. As shown in the inset, there are no trapping signals in the spectra for 0 V/-0.5 V and -0.5 V/-1.5 V, and thus the top GaAs layer is free of traps. This misfit-related trap has emission energy (capture cross section) of 0.35 eV (5.5×10^{-17} cm^2). Note that the trap peak in figure 8 is superimposed upon a continuous broad background signal at low temperatures. This broad signal may come from the electron emission from the QD states as observed in the C–V profiling. This is supported by the absence of this signal in the non-relaxed samples, consistent with a very short emission time for the QD. The peak intensity of this misfit-related trap is found to increase and finally saturate with increasing filling pulse time. This saturation suggests an exponential function for its capacitance–time transience, as previously observed [17]. This is characteristic of isolated point defects, rather than threading dislocations which display a logarithmic function [25, 26]. This trap was previously observed at 0.395 eV by Uchida *et al* [15] in relaxed InGaAs/GaAs quantum well structures. The DLTS spectra show a saturation of the peak intensity at $\Delta C = 0.3$ pF, which yields a sheet density about 2.5×10^9 cm^{-2} from $N_T = N_D(\Delta C/C_0^2)\varepsilon A$, where $N_D = 1 \times 10^{17}$ cm^{-3}, $C_0 = 300$ pF, area $A = 5 \times 10^{-3}$ cm^2 and permittivity $\varepsilon = 1.14 \times 10^{-10}$ F m^{-1}. This concentration is approximately one order of magnitude less than the QD density and is two orders of magnitude less than the misfit density ($\sim 2.4 \times 10^{11}$ cm^{-2}) observed in the bottom GaAs layer. This result suggests that only about 1% of the misfits are effective electron traps. A similar result was previously observed in relaxed InAsSb QDs [17]. This result is also consistent with the misfits in the QD which do not completely deplete the free electrons in the QD. In view of this carrier depletion, strain relaxation does not severely degrade the quality of the QD.

Convincing evidence for the tunneling-suppression model is provided by the previously reported relaxed InAsSb QD sample [17]. In this sample, without the InGaAs capping layer to relieve strain in top of the QD, strain relaxation is found to occur at the QD upper boundary, rather than at the QD bottom interface, and induce misfits in the QD and threading dislocations in the top GaAs layer. The GaAs bottom layer is free of misfits. This can be clearly seen in the TEM data in figure 1 of [17]. The carrier distribution reflects such a defect distribution. Figure 9 shows a weak quantum-emission QE peak in the QD at 0.27 μm and drastic carrier depletion in the front of the QD in the 20 K depth profile of this sample. The carrier distribution in the back of the QD is normal (with a valley concentration of 5×10^{16} cm^{-3}), consistent with there being no misfits in the bottom GaAs layer. Without the additional carrier depletion in the back of the QD, the QE peak displays no frequency-dependent dispersion even up to 10^5 Hz at 20 K, suggesting an emission time that is too short to be resolved. The long emission time and the additional carrier depletion in the back of the QD should be correlated. Hence, we believe that the increased emission time in the relaxed InAs/InGaAs QD sample is due to the suppression of tunneling by the additional carrier depletion in the GaAs bottom layer

related to the misfits. Due to the suppression of tunneling for the QD excited states, the electrons in the QD ground and first-excited states are thermally activated to the GaAs conduction band, allowing for the determination of the QD electronic band structure.

4. Conclusions

Strain relaxation is shown to induce additional carrier depletion in the GaAs bottom layer which can lengthen the emission time from the QD. The TEM data show the misfits in the QD and neighboring GaAs bottom layer. Thus, the misfits in the GaAs bottom layer may cause additional carrier depletion which can lengthen the emission time by the suppression of tunneling. As a result, the electrons in the QD states are thermally activated to the GaAs conduction band. This can explain the observed emission energies of 0.160 and 0.068 eV which are comparable to the confinement energies of the QD ground and first-excited states, respectively, with respect to the GaAs conduction band. DLTS reveals a trap at 0.35 eV in the bottom GaAs layer, which is attributed to the misfits. Its intensity is about two orders of magnitude less than the misfit intensity, suggesting that most of the misfits are not active traps.

Acknowledgments

The authors would like to thank the National Science Council of the Republic of China, Taiwan, for financially supporting this research under Contract No. NSC-95-2112-M-009-010. This work is partially supported by MOE ATU program.

References

[1] Heinrichsdorff F, Mao M H, Kirstaedter N, Krost A and Bimberg D 1997 *Appl. Phys. Lett.* **71** 22
[2] Eaglesham D J and Cerullo M 1990 *Phys. Rev. Lett.* **64** 1943
[3] Leonard D, Pond K and Petroff P M 1994 *Phys. Rev.* B **50** 11683
[4] Moison J M, Houzay F, Barthe F and Leprince L 1994 *Appl. Phys. Lett.* **64** 196
[5] Snyder C W, Mansfield J F and Orr B G 1992 *Phys. Rev.* B **46** 9551
[6] Shoji H, Mukai K, Ohtsuka N, Sugawara M, Uchida T and Ishikawa H 1995 *IEEE Photon. Technol. Lett.* **7** 1385
[7] Yusa G and Sakaki H 1996 *Electron. Lett.* **32** 491
[8] Campbell J C, Huffaker D L, Deng H and Deppe D G 1997 *Electron. Lett.* **33** 1337
[9] Kapteyn C M A, Heinrichsdorff F, Stier O, Heitz R, Grundmann M and Werner P 1999 *Phys. Rev.* B **60** 14265
[10] Luyken R J, Lorke A, Govorov A O, Kotthaus J P, Medeiros-Riberro G and Petroff P M 1999 *J. Appl. Phys.* **74** 2486
[11] Chang W H, Chen W Y, Cheng M C, Lai C Y, Hsu T M, Yeh N T and Chyi J I 2001 *Phys. Rev.* B **64** 125315
[12] Letartre X, Stievenard D and Lanoo M 1991 *J. Appl. Phys.* **69** 7336
[13] Wang J S, Chen J F, Huang J L, Wang P Y and Guo X J 2000 *Appl. Phys. Lett.* **77** 3027
[14] Chen J F, Hsiao R S, Wang C K, Wang J S and Chi J Y 2005 *J. Appl. Phys.* **98** 013716
[15] Uchida Y, Kakibayashi H and Goto S 1993 *J. Appl. Phys.* **74** 6720
[16] Chen J F, Hsiao R S, Shih S H, Wang P Y, Wang J S and Chi J Y 2004 *Japan. J. Appl. Phys.* **43** L1150
[17] Chen J F, Hsiao R S, Huang W D, Wu Y H, Chang L, Wang J S and Chi J Y 2006 *Appl. Phys. Lett.* **88** 233113
[18] Chen J F, Chen N C and Chen Y F 2001 *IEEE Trans. Electron Devices* **48** 204
[19] Kim J, Wang L W and Zunger A 1998 *Phys. Rev.* B **57** R9408
Williamson A J, Wang L W and Zunger A 2000 *Phys. Rev.* B **62** 12963
[20] Brunkov P N, Patane A, Levin A, Eaves L, MainYu P C, Musikhin Yu G, Volovik B V, Zhukov A E, Ustinov V M and Konnikov S G 2002 *Phys. Rev.* B **65** 085326
[21] Pal D, Firsov D and Towe E 2002 *Physica* E **15** 6
[22] Adawi A M, Zibik E A, Wilson L R, Lemaitre A, Cockburn J W, Skolnick M S, Hopkinson M and Hill G 2003 *Appl. Phys. Lett.* **83** 602
[23] Kim E T, Chen Z and Madhukar A 2001 *Appl. Phys. Lett.* **79** 3341
[24] Raghavan S, Rotella P, Stintz A, Fuchs B, Krishna S, Morath C, Cardimona D A and Kennerly S W 2002 *Appl. Phys. Lett.* **81** 1369
[25] Wosinski T 1989 *J. Appl. Phys.* **65** 1566
[26] Watson G P and Ast D G 1992 *J. Appl. Phys.* **71** 3399